Development of steady-state electrical-heating fluorescence-sensing (SEF) technique for thermal characterization of one dimensional (1D) structures by employing graphene quantum dots (GQDs) as temperature sensors

2016 Nanotechnology 27 445706

(http://iopscience.iop.org/0957-4484/27/44/445706)

IOP Publishing Nanotechnology
Nanotechnology 27 (2016) 445706 (9pp) doi:10.1088/0957-4484/27/44/445706

Development of steady-state electrical-heating fluorescence-sensing (SEF) technique for thermal characterization of one dimensional (1D) structures by employing graphene quantum dots (GQDs) as temperature sensors

Xiang Wan[1], Changzheng Li[1], Yanan Yue[1], Danmei Xie[1], Meixin Xue[2] and Niansu Hu[1]

[1] School of Power and Mechanical Engineering, Wuhan University, Wuhan, Hubei 430072, People's Republic of China
[2] China Ship Development and Design Center, Wuhan, Hubei 430064, People's Republic of China

E-mail: yyue@whu.edu.cn

Received 20 June 2016, revised 11 August 2016
Accepted for publication 19 August 2016
Published 27 September 2016

Abstract

A fluorescence signal has been demonstrated as an effective implement for micro/nanoscale temperature measurement which can be realized by either direct fluorescence excitation from materials or by employing nanoparticles as sensors. In this work, a steady-state electrical-heating fluorescence-sensing (SEF) technique is developed for the thermal characterization of one-dimensional (1D) materials. In this method, the sample is suspended between two electrodes and applied with steady-state Joule heating. The temperature response of the sample is monitored by collecting a simultaneous fluorescence signal from the sample itself or nanoparticles uniformly attached on it. According to the 1D heat conduction model, a linear temperature dependence of heating powers is obtained, thus the thermal conductivity of the sample can be readily determined. In this work, a standard platinum wire is selected to measure its thermal conductivity to validate this technique. Graphene quantum dots (GQDs) are employed as the fluorescence agent for temperature sensing. Parallel measurement by using the transient electro-thermal (TET) technique demonstrates that a small dose of GQDs has negligible influence on the intrinsic thermal property of platinum wire. This SEF technique can be applied in two ways: for samples with a fluorescence excitation capability, this method can be implemented directly; for others with weak or no fluorescence excitation, a very small portion of nanoparticles with excellent fluorescence excitation can be used for temperature probing and thermophysical property measurement.

Keywords: fluorescence, thermal property, graphene quantum dots, one dimensional, steady-state

(Some figures may appear in colour only in the online journal)

1. Introduction

Several measurement techniques have been developed in the past two decades to measure the thermophysical properties of one-dimensional (1D) materials, such as the 3ω method [1, 2], the microfabricated suspended device method [3, 4], the transient electro-thermal (TET) technique [5, 6] and the Raman-based thermal characterization technique [7, 8]. In the 3ω method, the second-harmonic temperature response of a sample is generated by a sine/cosine current. The amplitude and phase shift of the voltage variation at the third-harmonic frequency across the sample is used to determine thermophysical properties [1, 2]. The micro-bridge method measures the temperature difference of the sample between two electrodes, and, combined with heat transfer along the sample, the thermal conductivity of the sample can be characterized [3, 4]. The TET technique monitors the transient thermal response of the sample when heated by a step DC current. Thermal diffusivity and conductivity can be obtained through fitting the transient period of the temperature rise and is calculated from the steady-state curve respectively [5, 6].

The above referenced techniques are electrical thermal characterization methods which depend on the Joule heating of either the characterization device or sample. The fabrication of the electric circuit is a prerequisite, and the temperature determined from the resistance-temperature relationship is sometimes unstable and varies upon the different experimental setup, while a laser-based optical technique features non-contact and non-destructive measurement. Sometimes, the combined use of the electrical and optical method is advocated, e.g. the electrical heating combined with the optical temperature sensing technique. In 1D thermal characterizations, Raman spectroscopy has been widely used for temperature probing and thermal property measurement [7, 9, 10]. Yue *et al* developed a steady-state electro-Raman-thermal (SERT) technique for measuring the thermal conductivity of mircro/nanowires [7]. In the SERT technique, a sample is suspended between two electrodes and heated by DC currents. The middle-point temperature of the sample is probed by the Raman spectrum. The thermal conductivity of the sample can be obtained from the linear relationship between the middle-point temperature and the Joule heating energy. The SERT technique has been successfully applied on the thermal characterization of a carbon nanotube (CNT) bundle, fiber and buckypaper [7, 8, 11, 12]. It needs to be noted that the Raman signal has a non-elastic scattering effect in a laser-material interaction, and is often very weak for most materials. For materials which are not active in Raman excitation, the SERT technique is not applicable and this greatly limits the measurement capacity.

Fluorescence is another spectroscopy technique which advances a much stronger signal and the signal is temperature dependent [13–15]. Fluorescence thermometry has been used extensively for temperature probing or mapping [16–21]. Okabe *et al* demonstrated the intracellular temperature mapping based on fluorescence lifetime imaging microscopy [16]; Donner *et al* used green fluorescent proteins as thermal probes for intracellular temperature mapping [17]; Maruyama *et al* successfully measured the thermal conductivity of a single CNT using a fluorescent temperature sensor embedded in the electrodes [18]. Compared with Raman thermometry, the fluorescence spectrum not only features a stronger signal intensity but also has better temperature response [22–24]. For example, it was found that the temperature dependence of the fluorescence intensity of graphene quantum dots (GQDs) is significant [22]. Therefore, fluorescence spectroscopy can be used for thermophysical property measurement accordingly.

In this work, we develop a thermal characterization method based on fluorescence spectroscopy. Similar to the SERT technique, the steady-state electrical-heating fluorescence-sensing (SEF) technique also employs Joule heating and is capable of measuring the thermal conductivity of 1D materials. Compared with Raman thermometry where the to-be-measured material needs to be Raman active, this SEF method can be applied on any material, even without fluorescence excitation characteristics. Since small structures, such as QDs, have a very strong fluorescence effect [22–26], they can be used as the thermal probe coating on the to-be-measured material with weak or no self-excited fluorescence signal for thermal characterization, ideally without affecting its intrinsic thermal property.

2. Experimental principle and physical model

In the SEF method, a sample is suspended between two electrodes on a stage which is placed inside a vacuum chamber to reduce convective heat transfer. The schematic of the experimental setup for the SEF technique is shown in figure 1. During the measurement, the sample is fed with a constant current for steady-state Joule heating. The heat dissipates along the sample to the electrodes. As the heat sinks, the electrodes are required to be much larger than the sample, and the thermal contact resistance between them should be small. Therefore, the end temperature of the sample is regarded as room temperature during Joule heating.

The physical model of the SEF technique can be readily developed and the theoretical temperature distribution along the sample is shown in figure 1. Given that the distance from any point to the middle point of the sample is x, and the total length of the sample is $2\,\mathrm{L}$, a governing equation for heat conduction can be mathematically expressed as $\mathrm{d}^2T/\mathrm{d}x^2 = Q/(2\,\mathrm{L}{\cdot}k{\cdot}A_\mathrm{c})$, where k and A_c are the thermal conductivity and cross-sectional area of the sample, respectively. Herein, Q is equal to heating power $I^2{\cdot}R$, where I is the current and R is the resistance of the sample. Applied with boundary conditions $\mathrm{d}T/\mathrm{d}x|_{x=0} = 0$ and $T(L) = T_0$ (T_0 is the room temperature), the temperature distribution of the sample can be obtained as

$$T(x) = \frac{I^2RL}{4kA_c}\left(1 - \frac{x^2}{L^2}\right) + T_0 \qquad (1)$$

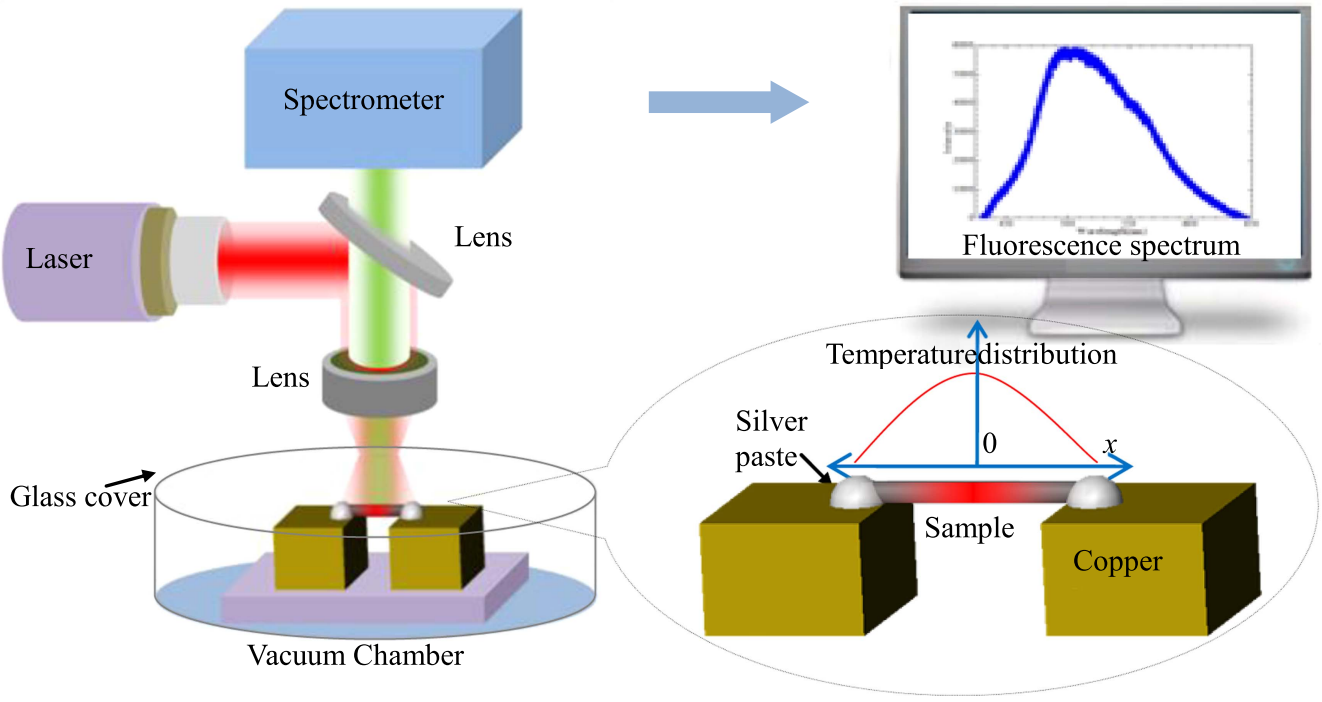

Figure 1. Schematic of the experimental setup of the SEF technique. The sample is suspended between two electrodes inside a vacuum chamber. The sample is heated by different constant currents and a violet lamp with a wavelength of 405 nm is used as the excitation source. The corresponding florescence signal is collected at each heating current.

The average temperature can be calculated as

$$\overline{T} = \frac{I^2RL}{6kA_c} + T_0 \tag{2}$$

The thermal conductivity of the sample can be derived from the slope of the $I^2{\cdot}R$–T curve.

If the sample itself is a good fluorescence agent, the strong fluorescence signal from the whole sample surface (the size of the sample is smaller than the laser spot) when irradiated with a laser can be used for temperature measurement. In this case, equation (2) can be directly employed for thermal conductivity calculation. If the size of the sample is larger than the laser spot, it needs to carefully focus the laser spot on the middle of the sample and integrate equation (1) between the middle point and half-length of the laser spot. For a sample with weak or no self-excited fluorescence signal, some nanoscale materials with good fluorescence excitation characteristics, such as QDs, should be used as the fluorescence agent for thermal probing. In such a case, the probing material can be coated or attached on the sample surface and the measured fluorescence signal represents the local temperature of the sample. If the sample is fully covered by the fluorescence agent, the average temperature of the sample can be obtained.

When the coating material is positioned only at the middle point of the sample or the sample is large enough compared with the size of the laser spot, the middle point temperature of the sample can be derived as

$$T(0) = \frac{I^2RL}{4kA_c} + T_0 \tag{3}$$

which is a little different from the average temperature equation (equation (2)). It is also found that the middle point temperature behaves with a linear relationship to the heating power, and the coefficient is $L/(4k{\cdot}A_c)$. As both the length and cross-sectional area of the sample are constant values, the thermal conductivity of the sample can be calculated from the slope of the $I^2{\cdot}R$–T curve. In these physical models, the laser energy absorbed by the sample is far less than the Joule heating energy, and Joule heating is considered as the heating source. In the measurement experiments, the laser irradiation is kept steady and the heating effect is consistent during the measurement. Thus the temperature increase induced by the laser heating effect should be the same. Since the slope of the $I^2{\cdot}R$–T curve is used to fit the thermal property instead of the individual point, the same temperature rise due to the heating effect does not affect the final result. Besides, to prevent an additional heating effect induced from the laser, extra caution on optical adjustment should be made to allow the lowest laser energy to excite the sound fluorescence signal to be detected.

3. Experimental details

To test the measurement capacity and accuracy of this technique, we select a standard material—platinum wire—for the measurement. As shown in figure 2(c), the length of the platinum wire is 6.2 mm, and the diameter is 25 μm. Since platinum is not the fluorescence agent, a supplemented material is needed to monitor its temperature during the heating

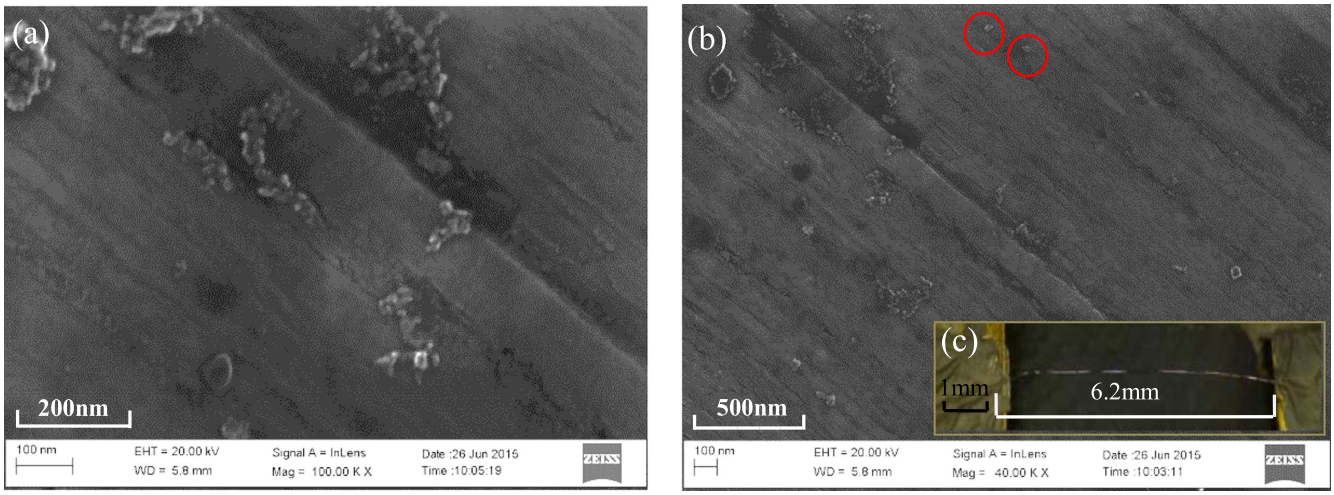

Figure 2. (a) and (b) are SEM images of the platinum wire with GQDs attached on the surface. The images show that GQDs are distributed on the platinum wire randomly and the size of the GQDs are much smaller compared with the sample. (c) The dimension of the sample measured in this experiment. The length of the platinum wire is 6.2 mm and the diameter is 25 μm.

experiment. GQDs are chosen as the supplemented material due to their nanometer scale and excellent fluorescence excitation property [22]. In the preparation procedure, the platinum wire is immersed into the GQDs solution thoroughly for about 12 h, and then it is air-dried at room temperature for 24 h. After repeating the process three times, it is assumed that the GQDs are attached on the surface of the platinum wire uniformly. Figures 2(a) and (b) are the scanning electron microscopy (SEM) images of the sample, showing that these GQDs on the surface of the platinum wire are randomly distributed. In figure 2(b), there are some single GQDs distributed separately on the platinum wire surface. It can be found that the size of GQDs is much smaller compared with the platinum wire.

In our past work, we found that the intensity, peak shift and peak width of fluorescence in GQDs have a significant temperature effect [22]. The fluorescence intensity decreases over 50% when the temperature rises from 5 °C–80 °C, which is more significant than conventional semiconductor QDs [23–26]. Comparably, the fluorescence bandwidth is much wider in GQDs [27]. As a carbon material, GQDs can be highly soluble in sundry solvents and equipped with functional groups at their edges. Thus GQDs are generously available for most applications compared with semiconductor QDs [28]. The temperature dependence of the peak shift and peak width is not as significant as that of the peak intensity due to the uncertainty in data processing. Therefore, the fluorescence intensity is chosen to analyze the temperature evolution in the experiment. In the temperature-normalized intensity calibration experiment, the environmental temperature and corresponding fluorescence spectra of GQDs are recorded. Before each signal acquisition, the sample is maintained for 5 min at each temperature to guarantee that the sample has reached the steady state. The fluorescence spectra are recorded three times at each temperature for averaging to ensure accuracy. In the temperature coefficient calibration experiment, strong fluorescent emissions are observed by the spectrometer. Figure 3(a) shows the temperature dependence of the fluorescence spectrum intensity of GQDs. It can be seen that the fluorescence intensity of GQDs decreases with increasing temperature, almost 60% for the temperature range of 70 °C. In figure 3(b), the normalized fluorescence spectrum intensity shows a linear relationship with temperature with a slope $-0.0088\ \mathrm{K}^{-1}$. Since the GQDs' distribution for each platinum wire with GQDs covered are different, the coefficient of the normalized fluorescence spectrum intensity with respect to temperature might change. To ensure accuracy, it is suggested that the calibration experiment for each sample is conducted before using this SEF technique.

In the measurement experiment, the sample stage is placed in a vacuum chamber to minimize convective heat transfer. Two large copper pieces used as electrodes are connected to the power supply. Two ends of the platinum wire are attached to the copper pieces by silver paste, and the electrical resistance of the wire is 1.75 ohms. Due to the high thermal conductivity of the silver paste, electrical/thermal contact resistance between the wire and copper pieces can be neglected. Since the copper pieces have good thermal conductivity and the volume is much bigger than the sample, the sample endpoint temperature can be regarded as room temperature. The wire is heated under different constant currents supplied by a current source (KEITHLEY 6220) from 5 mA–55 mA. The GQDs used in this work are purchased from ACS Materials Company and are synthetized via the bottom-up method [29–31]. According to the information from the supplier, GQDs with controllable morphologies are produced by the bottom-up method from small carbon precursors, such as glucose and citric. GQDs have a well-distributed size of 15 nm and a quantum yield of 7 ~ 11%. The standard concentration of GQDs water solution is $1\ \mathrm{mg}\cdot\mathrm{ml}^{-1}$. In our experiment, a laser with a wavelength of 405 nm is used as the excitation light source and the energy density of the laser beam is $0.38\ \mathrm{mW\ mm}^{-2}$. By accounting for the irradiation area of the sample and the absorptivity of

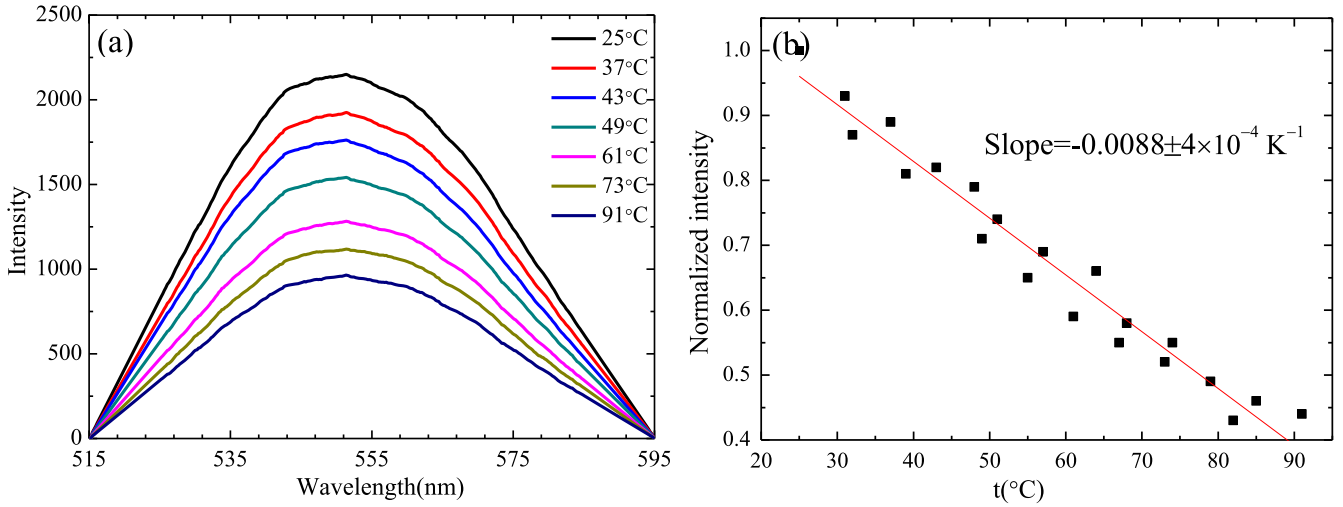

Figure 3. (a) Fluorescence spectra of GQDs at different temperatures from 25 °C–91 °C in the calibration experiment. It shows that the intensity decreases with increasing temperature and there is not an obvious peak shift due to the wide spectrum. The normalized intensity is used as the temperature indicator in this experiment. (b) The linear fitting of normalized intensity with respect to temperature.

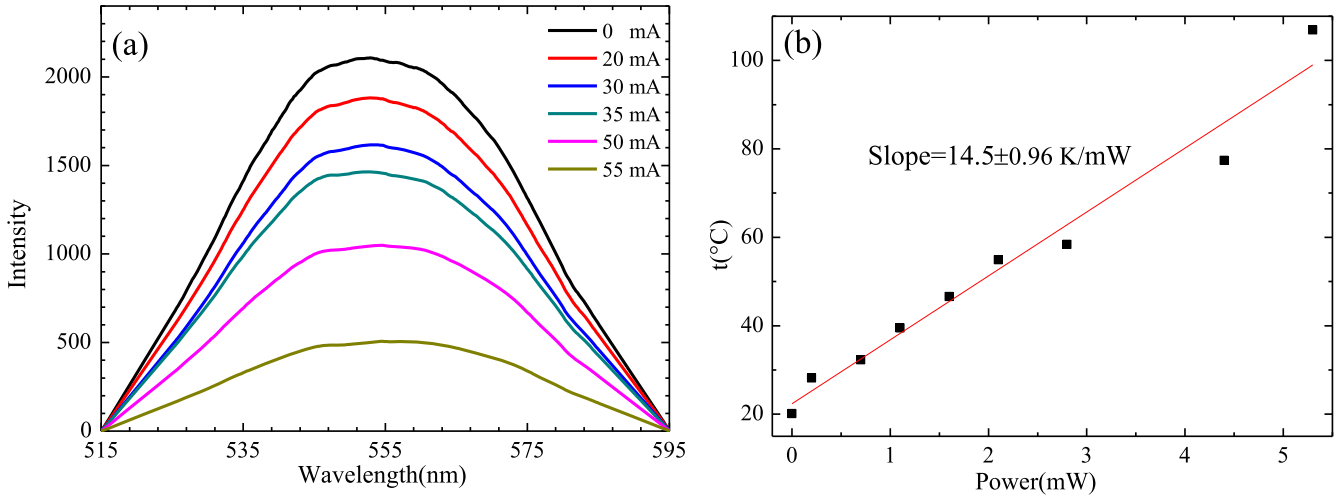

Figure 4. (a) Different fluorescence spectrum of GQDs attached on the platinum wire when heated under different currents from 0 mA–55 mA. The temperature of the sample increases according to increased heating power. The excited fluorescence signal from GQDs at the sample surface represents the sample temperature.(b) The linear fitting result of the sample temperature (obtained from the fluorescence intensity in figure 4(a)) with respect to the heating power.

platinum wire at a wavelength of 405 nm, the absorbed laser energy is only 0.02 mW, which is much less than the current energy (from 0.2 mW–5.3 mW) in the experiment. It has been proven that the GQDs sample exhibited a great florescence signal under such violet light excitation [22]. All excitation spectra and fluorescent decays are recorded by an Ocean Optics HR2000+ spectrometer.

The platinum wire we use is a standard material; the thermal diffusivity and thermal conductivity is $2.52 \times 10^{-5}\,\mathrm{m^2\,s^{-1}}$ and $71.6\,\mathrm{W/(m^{-1}\cdot K)}$, respectively [5]. In the SEF measurement, the wire is heated by a different constant current. The size of the laser spot is adjusted to be much larger than the sample so that the sample can be completely covered by the laser and guarantee that the fluorescence signal of the GQDs comes from the total surface of the wire. This ensures that the measured temperature represents the average temperature of the sample. Before each signal acquisition, the sample is maintained for 5 min at each constant current to guarantee that the sample has reached the steady state. The data is collected three times at each current for averaging to ensure accuracy.

4. Results and discussion

4.1. Experimental results

Figure 4(a) shows the power dependence of the fluorescence intensity; as Joule-heating power increases, the temperature of the wire/GQDs increases, and the fluorescence spectrum intensity decreases. By the linear relationship between the normalized fluorescence spectrum intensity and temperature, $y = -0.0088x + 1.18$, the temperature corresponding to the

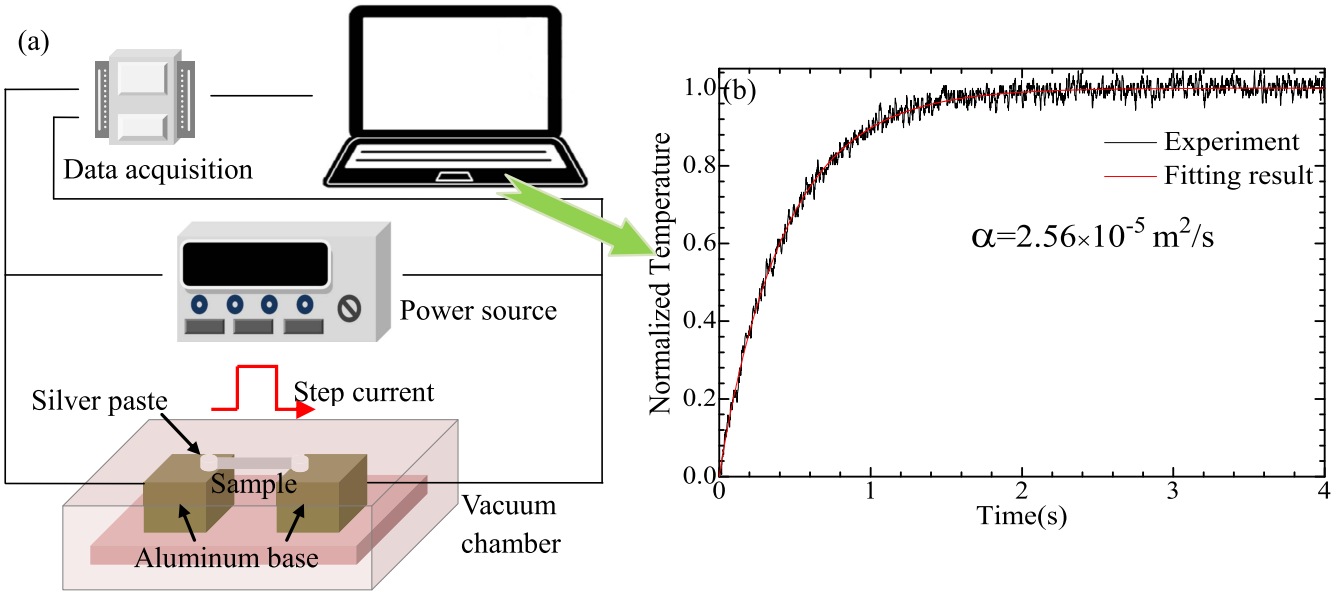

Figure 5. (a) Schematic of experimental setup for the TET experiment. The sample is suspended between two electrodes in a vacuum chamber. Under Joule heating with a step DC current, the sample experiences the transient temperature increase until it reaches a steady state. The temperature variation can be monitored by recording the voltage over the sample as the electrical resistance and temperature are correlated. (b) An example data for normalized temperature with respect to time. Thermal diffusivity can be determined as $2.56 \times 10^{-5}\,\mathrm{m^2\,s^{-1}}$ by fitting this curve.

normalized fluorescence spectrum intensity can be calculated. The heating power–temperature curve is shown in figure 4(b), and the slope of the temperature with respect to the heating power is $14.5\,\mathrm{K\,mW^{-1}}$ by fitting. According to equation (2), the slope is the value of $L/(6k{\cdot}A_c)$. As L and A_c are all constant values, then k can be calculated as $72.6 \pm 4.8\,\mathrm{W/(m \cdot K)}$. Compared with the standard value of $71.6\,\mathrm{W/(m \cdot K)}$, the error is less than 1.5%.

4.2. Effect of GQDs on thermal property measurement

When using coated material as the fluorescence agent, it is essential that the coating material cannot affect the intrinsic property of the measuring material. Therefore, only a small dose can be used. In this work, we use the GQDs, which are excellent in fluorescence excitation and have a negligible effect on thermal property measurement. To confirm this, we conduct a parallel measurement on the platinum wire by using the TET technique. The TET technique has been proven to be a convenient and effective approach for measuring thermal diffusivity and conductivity of microwires [5, 6]. The schematic is as shown in figure 5(a): a to-be-measured sample is suspended between two electrodes in a vacuum chamber. The sample is fed with a step DC current, and its temperature increases until it reaches the steady state. The temperature rise of the sample causes the variation of electrical resistance. Thus the temperature evolution can be obtained by measuring the voltage evolution during the heating period. Thermal diffusivity ($\alpha = k/\rho c_p$) of the sample can be calculated by fitting the time–temperature curve using the equation [5]:

$$T^* = \frac{96}{\pi^4}\sum_{m=1}^{\infty}\frac{1 - \exp[-(2m-1)^2\pi^2\alpha t/L^2]}{(2m-1)^4} \qquad (4)$$

where $T^* = (T(t) - T_0)/(T(t \to \infty) - T_0)$ is the normalized temperature increase. Thermal conductivity can be derived from the temperature increase as $k = q_0L^2/12\Delta T$. In the TET experiment, as shown in figure 5(b), the thermal diffusivity of the wire with GQDs is calculated as $2.56 \times 10^{-5}\,\mathrm{m^2\,s^{-1}}$. The thermal conductivity is obtained to be $72.8\,\mathrm{W/(m \cdot K)}$. Comparably, thermal diffusivity and thermal conductivity of the wire without GQDs is calculated as $2.52 \times 10^{-5}\,\mathrm{m^2\,s^{-1}}$ and $71.6\,\mathrm{W/(m \cdot K)}$, respectively. The effect of GQDs causes only 1.7% error in the thermal conductivity measurement, and this error can be diminished by using a smaller dose of GQDs. It is noteworthy that when measuring extremely small materials, e.g. samples at nanoscale, the intrinsic property of fluorescence excitation is needed for the sample rather than by coating additional materials, since it could be a factor that influences the measurement accuracy. Owing to the nanoscale size of GQDs and the micro-to-millimeter scale of the sample we used in this SEF technique, the intrinsic thermal property of the sample is not impacted too much by these GQDs.

4.3. Experimental uncertainty analysis

The uncertainty of the measurement result mainly comes from three factors: uncertainty induced by the linear fitting during data processing, laser heating effect and heat loss. The thermal conductivity of the wire is obtained as $72.6 \pm 4.8\,\mathrm{W/(m \cdot K)}$. The uncertainty of $4.8\,\mathrm{W/(m \cdot K)}$ is from the linear fitting process, which can be improved by performing several measurements at the same current. If more data points are collected during the experiment, the linearity of these data points may be more obvious, and the uncertainty value can be

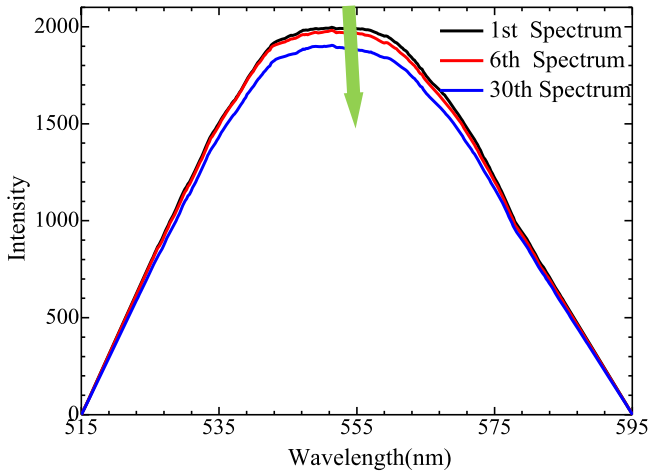

Figure 6. Collected fluorescence spectrum of GQDs after a much longer laser irradiation compared with laser excitation integration time in the SEF experiment. The total irradiation time is 30 times that of the integration in the SEF experiment. It can be seen the fluorescence intensity decreases with the laser on. However, this peak intensity reduction is indistinctive. Comparing the black line (1st spectrum) with the red line (6th spectrum), the two lines nearly overlap. In comparison, the decrease of the fluorescence intensity is not obvious until the 30th spectrum collection. Even so, fluorescence intensity decreases by only 5% of the total intensity.

reduced further. For the laser heating, as analyzed above, the wire is completely covered by the laser spot during the experiment. The laser heating effect on the sample is kept consistent. Thus, the temperature rise induced by the laser heating effect should be the same. In our data processing, only the slope of the temperature–power curve is used where the same temperature increase does not affect the final result. Moreover, the heating effect from the laser is adjusted to be as weak as possible by adjusting the focal level of the configuration while ensuring a sound fluorescence signal.

The fluorescence quenching effect, which refers to the decreased intensity when irradiated with a laser beam, is often observed in common fluorescence agents. The quenching effect is a complex process which is caused by many physical factors, one of which is the high laser intensity induced shifting effect. In this work, we need to exclude or minimize the effect of the quenching effect of GQDs on the reduced fluorescence intensity, which will deliver an error in temperature transformation. To achieve this, we minimize the laser intensity as much as possible during the measurement. To confirm this operation, we take the fluorescence spectrum without Joule heating after an acquiring time 29 times longer than the time we use in the SEF experiment, and compare this spectrum with the spectrum from instant laser irradiation. In figure 6, the sample is heated by the laser energy individually. The 1st spectrum, 6th spectrum, and the 30th spectrum are the spectrum collected during the first, sixth, and the thirtieth round of the integration time, respectively. The temperature increase induced fluorescence intensity drop due to the quenching effect is involved in the measurement. In the 6th spectrum, the laser heating effect is six times that of the 1st spectrum. It is found that there is not much difference between them. In the 30th spectrum, the laser heating effect is 30 times that of the 1st spectrum; the fluorescence intensity decreases only 5% than the original spectrum after a long-time laser irradiation. It can be concluded that the temperature increase due to the quenching effect is not significant in our experimental setup. Furthermore, the laser irradiation time during our experiment is carefully controlled to the minimum so that the quenching effect is further reduced and has a negligible effect on our measurement uncertainty.

In the measurement, the heat loss can be another factor introducing uncertainty. The heat loss includes the radiation heat loss and convective heat loss. Since the experiment is performed in a vacuum chamber, convective heat loss can be neglected and only radiation heat loss needs to be considered. The radiation heat loss can be roughly estimated by the thermal radiation formula $\Phi = \varepsilon\sigma A(T^4\text{-}T_0^4)$, where ε is emissivity (taken as 1 for the maximum calculation), σ is the blackbody radiation constant, which is taken as $5.67 \times 10^{-8}\,\mathrm{W/(m^2 \cdot K^4)}$, A is the surface area of the wire. The largest radiation heat loss of the wire is calculated at the highest temperature as 0.37 mW, and the corresponding heating power is 5.3 mW; thus the portion of radiation heat loss is about 6.9%. In our measurement, aluminum-foil was used to cover the vacuum chamber to minimize the radiation heat loss. Therefore, the radiation heat loss contributes very little uncertainty in the measurement.

4.4. Advantage of SEF technique and extended application

Compared with a Raman signal, a fluorescence spectrum signal is much more significant and the integration time needed for each spectrum acquisition is much shorter. Moreover, due to the fact that GQDs are low-toxic and bio-compatible [32], this new SEF method is promising for the thermal characterization of bio-materials. Besides, as an optical measurement method, the SEF method features steady state measurement instead of transient measurement in most conventional laser-based thermal characterization techniques (such as laser flash and pump-probe, etc). Therefore, this SEF method features an easy and fast measurement, and should have a wide range of implementations.

The SEF technique can be modified for measuring the thermal property of nonconductive materials by using laser heating after adjusting the physical model slightly. The schematic is shown in figure 7. The sample configuration is almost the same: the sample is suspended between two electrodes, and two ends of the sample are connected to the two electrodes with silver paste respectively. A laser is focused on the middle region of the sample. In the new model, the governing equation for heat transfer in the laser irradiation region can be determined as $\mathrm{d}^2T/\mathrm{d}x^2 + q/k = 0$. Herein, T is temperature, x is the coordinaqte along the sample with its middle point which is regarded as the original point, k is the thermal conductivity of the sample, q is the equivalent heat generation rate, $q = Q/(2\pi r_s^2 r_0)$, where Q is the absorbed laser energy, r_s is the radius of the sample, r_0 is the half length of the laser beam. Outside the laser irradiation region, a governing equation without an inner heat source can

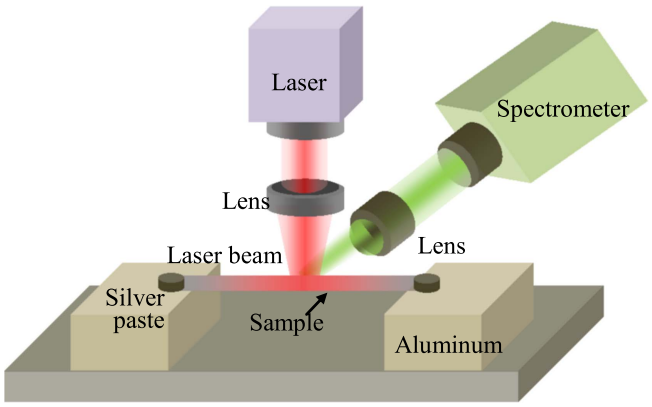

Figure 7. Schematic of the experimental setup of laser heating and fluorescence sensing for thermal characterization. A sample is suspended between two aluminum bulks, and a laser, which is used as a heating and excitation source, is focused on the middle area of the sample. When heated by laser energy, heat dissipates from the laser irradiation region to the ends of the sample. The average temperature of the laser irradiation region can be obtained by analyzing the florescence signal, and the thermal conductivity of the sample can be derived.

be described as

$$\frac{k\Delta T\pi r_s^2}{L - r_0} + \frac{Q}{2} = 0 \tag{5}$$

In this equation, L is the half length of the sample. Thus temperature $T(r_0)$ can be calculated as $Q(L\text{-}r_0)/(2\pi r_s^2 k) + T_0$ (T_0 is room temperature) by the governing equation outside the laser irradiation region. Considering the two boundary conditions $\mathrm{d}T/\mathrm{d}x|_{x=0} = 0$ and $T(r_0) = Q(L\text{-}r_0)/(2\pi r_s^2 k) + T_0$, the average temperature at the laser heating region can be derived as

$$\overline{T} = \frac{QL}{2k\pi r_s^2} - \frac{Qr_0}{3k\pi r_s^2} + T_0 \tag{6}$$

There exists a linear correlation between the average temperature and the laser energy. In the measurement, the laser energy should be set from weak to strong, thus the thermal conductivity can be derived from the slope of the Q–T curve.

5. Conclusions

In this work, an optical method designated SEF technique based on fluorescence thermometry and Joule heating is developed to measure the thermal conductivity of micro/nanowires. To implement this technique, the sample needs to be either fluorescence active or small particles used as the fluorescence agent for temperature probing. As a demonstration, a platinum wire is tested by using this SEF technique and GQDs are used as the fluorescence agent coating on the wire for exciting the fluorescence signal. Based on the 1D heat conduction model, the thermal conductivity of platinum wire is measured to be 72.6 $\mathrm{W/(m \cdot K)}$, which is close to the standard value from reference. TET experiments conducted on the same platinum wires validate that the coating with a small dose of GQDs has a negligible effect on the sample's thermal property. Therefore, it is viable to use a fluorescence agent on the sample when employing the SEF technique in thermal characterizations. Compared with the large uncertainty and low signal intensity of Raman thermometry, this SEF technique has a much wider range of applications, and is capable of measuring both fluorescence active and non-active, conductive and non-conductive materials, especially biomaterials.

Acknowledgments

The financial support from the National Natural Science Foundation of China (Nos. 51428603 and 51576145) is gratefully acknowledged.

References

[1] Cahill D G 1990 Thermal conductivity measurement from 30 to 750 K: the 3 Omega method *Rev. Sci. Instrum.* **61** 802–8
[2] Frank R, Drach V and Fricke J 1993 Determination of thermal conductivity and specific heat by a combined 3ω/decay technique *Rev. Sci. Instrum.* **64** 760–5
[3] Kim P, Shi L, Majumdar A and Mceuen P 2001 Thermal transport measurements of individual multiwalled nanotubes *Phys. Rev. Lett.* **87** 215502
[4] Shi L, Li D, Yu C, Jang W, Kim D and Yao Z 2003 Measuring thermal and thermoelectric properties of one-dimensional nanostructures using a microfabricated device *J. Heat. Trans.* **125** 881–8
[5] Guo J, Wang X and Wang T 2007 Thermal characterization of microscale conductive and nonconductive wires using transient electrothermal technique *J. Appl. Phys.* **101** 63537
[6] Li M, Sun Y, Xiao H, Hu X and Yue Y 2015 High temperature dependence of thermal transport in graphene foam *Nanotechnology* **26** 105703
[7] Yue Y, Eres G, Wang X and Guo L 2009 Characterization of thermal transport in micro/nanoscale wires by steady-state electro-Raman-thermal technique *Appl. Phys.* A **97** 19–23
[8] Li M and Yue Y 2015 Raman-based steady-state thermal characterization of multiwall carbon nanotube bundle and buckypaper *J. Nanosci. Nanotechnol.* **15** 3004-10
[9] Kearney S P, Phinney L M and Baker M S 2006 Spatially resolved temperature mapping of electrothermal actuators by surface Raman scattering *J. Microelectromech. Syst.* **15** 314–21
[10] Balandin A A, Ghosh S, Bao W, Calizo I, Teweldebrhan D, Miao F and Lau C N 2008 Superior thermal conductivity of single-layer graphene *Nano Lett.* **8** 902–7
[11] Li Q, Liu C, Wang X and Fan S 2009 Measuring the thermal conductivity of individual carbon nanotubes by the Raman shift method *Nanotechnology* **20** 145702
[12] Yue Y, Huang X and Wang X 2010 Thermal transport in multiwall carbon nanotube buckypapers *Phys. Lett.* A **374** 4144–51
[13] Amdursky N, Gepshtein R, Erez Y and Huppert D 2011 Temperature dependence of the fluorescence properties of Thioflavin-T in propanol, a glass-forming liquid *J. Phys. Chem.* A **115** 2540–8
[14] Yu P, Wen X, Toh Y and Tang J 2012 Temperature-dependent fluorescence in carbon dots *J. Phys. Chem.* C **116** 25552–7

[15] Le-Van Q, Roux X, Teperik T, Habert B and Marquier F 2015 Temperature dependence of quantum dot fluorescence assisted by plasmonic nanoantennas *Phys. Rev.* B **91** 85412
[16] Okabe K, Inada N, Gota C, Harada Y, Funatsu T and Uchiyama S 2012 Intracellular temperature mapping with a fluorescent polymeric thermometer and fluorescence lifetime imaging microscopy *Nat. Commun.* **3** 705
[17] Donner J S, Thompson S A, Kreuzer M P, Baffou G and Quidant R 2012 Mapping intracellular temperature using green fluorescent protein *Nano Lett.* **12** 2107–11
[18] Maruyama H, Kariya R and Arai F 2013 Evaluation of thermal conductivity of single carbon nanotubes in air and liquid using a fluorescence temperature sensor *Appl. Phys. Lett.* **103** 161905
[19] Yue Y and Wang X 2012 Nanoscale thermal probing *Nano Rev.* **3** 11586
[20] Brites C D S, Lima P P, Silva N J O, Millán A, Amaral V S, Palacio F and Carlos L D 2010 A luminescent molecular thermometer for long-term absolute temperature measurements at the nanoscale *Adv. Mater.* **22** 4499–504
[21] Freddi S *et al* 2013 A molecular thermometer for nanoparticles for optical hyperthermia *Nano Lett.* **13** 2004–10
[22] Li C and Yue Y 2014 Fluorescence spectroscopy of graphene quantum dots: temperature effect at different excitation wavelengths *Nanotechnology* **25** 435703
[23] Walker G W, Sundar V C, Rudzinski C M, Wun A W, Bawendi M G and Nocera D G 2003 Quantum-dot optical temperature probes *Appl. Phys. Lett.* **83** 3555–7
[24] Li S, Zhang K, Yang J, Lin L and Yang H 2007 Single quantum dots as local temperature markers *Nano Lett.* **7** 3102–5
[25] Al Salman A, Tortschanoff A, Mohamed M B, Tonti D, van Mourik F and Chergui M 2007 Temperature effects on the spectral properties of colloidal CdSe nanodots, nanorods, and tetrapods *Appl. Phys. Lett.* **90** 93104
[26] Dai Q, Zhang Y, Wang Y, Hu M Z, Zou B, Wang Y and Yu W W 2010 Size-dependent temperature effects on PbSe nanocrystals *Langmuir* **26** 11435–40
[27] Pan D, Zhang J, Li Z and Wu M 2010 Hydrothermal route for cutting graphene sheets into blue-luminescent graphene quantum dots *Adv. Mater.* **22** 734–8
[28] Bacon M, Bradley S J and Nann T 2014 Graphene quantum dots *Part. Part. Syst. Charact.* **31** 415–28
[29] Yan X, Cui X and Li L 2010 Synthesis of large, stable colloidal graphene quantum dots with tunable size *J. Am. Chem. Soc.* **132** 5944–5
[30] Liu R, Wu D, Feng X and Mullen K 2011 Bottom-up fabrication of photoluminescent graphene quantum dots with uniform morphology *J. Am. Chem. Soc.* **133** 15221–3
[31] Lu J, Yeo P S E, Gan C K, Wu P and Loh K P 2011 Transforming C60 molecules into graphene quantum dots *Nat. Nanotechnology* **6** 247–52
[32] Zhu S *et al* 2011 Strongly green-photoluminescent graphene quantum dots for bioimaging applications *Chem. Commun.* **47** 6858–60